27 CALCULATING THE FRACTIONATION OF ISOTOPES IN HYDROCHEMICAL (TRANSPORT) PROCESSES WITH PHREEQC-2[1]

C.A.J. Appelo
Hydrochemical Consultant
Amsterdam, NL.
e-mail: appt@xs4all.nl

Abstract

Often, a single fractionation factor is used for calculating the separation and the concentration ratio of two isotopes in solution during transport. This is not correct, of course. The fractionation factor gives the concentration ratio of two isotopes among two phases *in equilibrium*. Actually, during transport coupled with reaction the ratios in the solution change and the isotope effect may enhance as distance increases. Similarly with diffusion, with or without reaction, the isotope separation is a function of distance and time.

The transport aspect in isotope separation is well known to show up in a progressive isotope lightening of rain generated from atmospheric vapor (in the Rayleigh fractionation process). The isotopes of other elements involved in reactions and transport generally do require computer models for proper evaluation because their fractionation also is affected by pH and complexation in solution. The computer model PHREEQC-2 was designed for hydrogeochemical calculations, but various features of the code enable to include isotopes as an integral part of the hydrogeochemical model. It is shown how the calculations can be done for the ratio of $^{18}O/^{16}O$ in rain condensing from vapor and for calcite precipitating under various conditions.

Fractionation during diffusion in the first instance appears to increase the separation among isotopes indefinitely with time. However, the fractionation of $^{37}Cl/^{35}Cl$ in natural waters does not exceed the range from about -1.5 to +1‰. The diffusion of the two Cl isotopes can also be modeled with PHREEQC-2. Furthermore, it is shown that the maximal fractionation during diffusion is limited when both the isotopes are present in the interdiffusing solutions. Thus, Cl isotope fractionation may not be a clear indicator of diffusion as the source of saline groundwater.

27.1 Introduction

Isotopes of an element behave slightly differently during evaporation, condensation, transport and/or reactions, processes which all lead to isotope fractionation (Clark and Fritz, 1997; Lasaga, 1998; Valley and Cole, 2001). Most simply, fractionation considers the ratio of two isotopes in two species or two phases at equilibrium, which implies that the ratio is constant among the phases or species. The ratio may grow and change 1) in separation processes where the product is removed from the reactant (Rayleigh fractionation), 2) with the progress of chemical reactions and 3) during diffusion. Rapidly, the calculations become complicated if these processes take place together and numerical models are necessary to bring relief (Bowers and Taylor, 1985; Lee and Bethke, 1996). Basically, the model is used to calculate the reactions, and a mass balance in

[1] Chapter 27 in H.D. Schulz and A. Hadeler (eds) Geochemical processes in soil and groundwater. GeoProc 2002, Wiley-VCH, Weinheim, p. 383-398. ***Note*** The pages were reformatted for this pdf file.

combination with isotope fractionation factors is employed to calculate the isotope concentrations in the rock and in water. Another approach is to include all the isotope species in the geochemical model and to calculate fractionation directly for the final overall compositions (Thorstenson and Parkhurst, 2002).

It is not the purpose of this contribution to model a specific dataset, but rather to show how various options of the hydrogeochemical computer program PHREEQC (Version 2) (Parkhurst and Appelo, 1999) can be invoked to calculate isotope fractionation. PHREEQC-2 was developed for hydrogeochemical calculations for equilibrium or kinetic reactions in batch or 1D flow systems, but the Runge-Kutta integration procedure of the code and the flexible input formats allow to calculate isotope fractionation as well. The first example simulates oxygen fractionation during condensation of vapor in a Rayleigh process, the next is about ^{13}C fractionation in precipitating calcite under varying conditions where the capabilities of PHREEQC-2 can be optimally implemented. The last example considers Cl isotope fractionation during diffusive transport.

27.2 Isotope fractionation and the Rayleigh process

The heavier molecule $H_2{}^{18}O$ condenses more readily from vapor than $H_2{}^{16}O$, producing liquid water that is isotopically heavier than the vapor. Thus, when a small number of dN molecules of light $H_2{}^{16}O$ condense, they are accompanied by dN_i molecules of heavy $H_2{}^{18}O$, but the ratio dN_i/dN in the condensate is higher than the ratio N_i/N in the vapor:

$$\frac{\mathrm{d}\,N_i}{\mathrm{d}\,N} = \alpha\,\frac{N_i}{N} \tag{1}$$

where α is the *fractionation factor* (no dimension).

With the isotope ratio $N_i/N = R$ and the initial values R_0 and N_0 we integrate Eq. (1) and obtain the Rayleigh formula:

$$\frac{R}{R_0} = \left(\frac{N}{N_0}\right)^{(\alpha - 1)} \tag{2}$$

With Eq. (2) we can calculate how R in atmospheric vapor changes during rain-out, as well as the isotopic ratio in the rain since this equals the ratio of the heavy and the light molecules which condense from the vapor. Or, with Eq. (1):

$$R_{\mathrm{rain}} = \mathrm{d}N_i\,/\mathrm{d}N = \alpha R_{\mathrm{vapor}} \tag{3}$$

To calculate the actual process in which vapor cools and condenses and α changes with temperature, requires numerical integration of (1). The kinetic integrator that was programmed in PHREEQC-2 can do this in several ways, and one is as follows. The condensation of 1 g $H_2{}^{16}O$ vapor can be calculated as a function of the temperature over the range from 25 to -20 °C as kinetic process, which provides stepwise values of d(^{16}O). For each step, the amount d(^{18}O) is calculated in another rate according to Eq. (1) while the Runge-Kutta procedure maintains the integration accuracy in accordance with a user-definable tolerance (default is 10^{-8} moles). We may look at the input files without considering details of the code which is now well established.

PHREEQC-2 processes input files in which keywords define the problem as explained in the user's manual of Parkhurst and Appelo (1999). These keywords are capitalized in the examples shown here. In Example 1, first a SOLUTION is defined, in this case plain water at 25°C. The REACTION_TEMPERATURE keyword circumscribes the temperature range and the number of steps by which it should change. The kinetic calculations are indicated under keyword RATES in the form of small programs in which special functions provide access to all the parameters of the chemical model. For example, the statement SR("H2O(g)") in line 10 of the rate 'Condense' gives the saturation ratio for H_2O (which equals the partial pressure of water vapor), and TK in

line 20 is the temperature in Kelvin. The rates are invoked with keyword KINETICS to set the initial mass 'm0' of the kinetic reactants, and thus also the initial amounts of the isotopes ^{16}O and

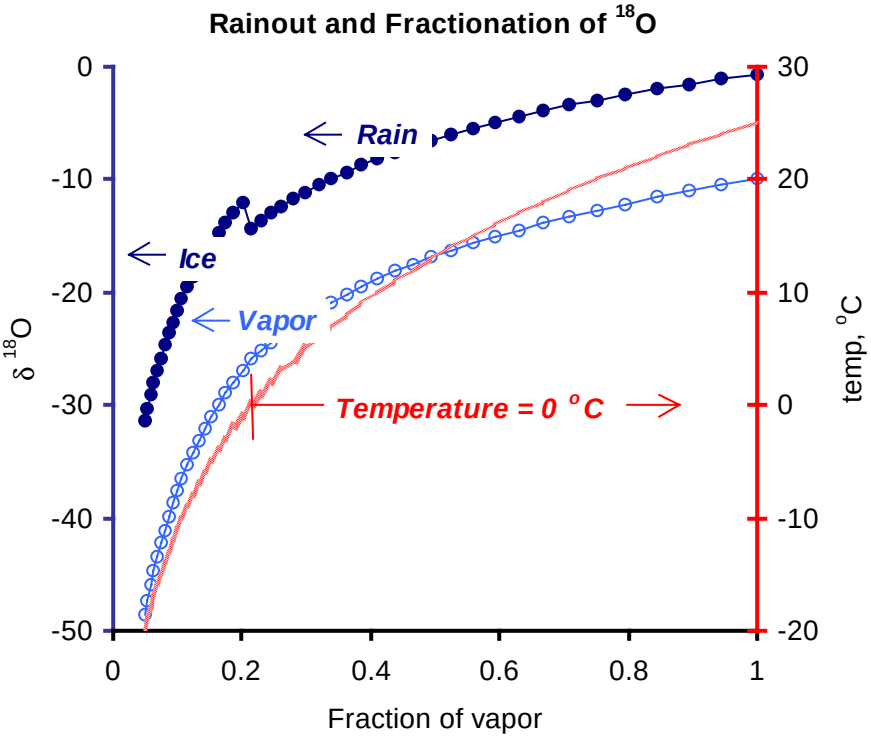

Figure 27.1. Fractionation of ^{18}O during cooling of water vapor from an initial temperature of 25 °C to -20 °C with condensation of rain and subsequently of ice. Initial $\delta^{18}O_{vapor}$ = -10‰.

^{18}O and thereby the isotope ratio in the initial vapor. The output of the program is lengthy, but can be confined to specific components in separate files, while the windows version (by Vincent Post, www.geo.vu.nl/users/posv/phreeqc.html) also permits to chart the results. In Figure 27.1, the chart shows the depletion of ^{18}O as rainout progresses and the fraction of vapor decreases. Note the jump of ^{18}O in Figure 27.1 at 0 °C, where the fractionation factor changes from vapor-liquid to vapor-ice. The fractionation factor is defined in lines 10 and 20 of the rate 'Frn_18O' according to Majoube (1971).

```
# Example 1 a # indicates comment
# Calculate 18O fractionation during condensation
SOLUTION 1
REACTION_TEMPERATURE
 25 -20 in 46 steps # change temp in 1 degree steps

RATES
 Condense
 -start
  10 P_eq = SR("H2O(g)")    # the vapor pressure
  20 n_eq = P_eq * 43.54165 / 0.082057 / TK     # n = PV/RT
  30 d16O = (m - n_eq) * time
  40 save d16O          # ... integrate
  50 put(d16O, 1)       # store d16O in temporary memory
 -end

 Frn_18O
 -start
```

```
  10 if TK > 273.15 then c = -2.0667e-3 else c = 1.0333e-3
  20 aa_l_v = exp(1.137e3/TK^2 - 0.4156/TK + c)       # Majoube, 1971
  30 d18O = aa_l_v * m / kin("Condense") * get(1)
  40 put(aa_l_v, 2)
  50 save d18O                      # ...integrate
 -end

KINETICS 1
 Condense; -formula H2O 0; m0 55.506e-3
 Frn_18O;  -formula H2O 0; m0 0.110177e-3       # d18O = -10 permil
 -steps 6
END
```

27.2.1 Fractionation during precipitation of minerals

PHREEQC-2 is particularly useful for including the effects of a changing hydrogeochemistry on isotope fractionation. For example, fractionation of ^{13}C in calcite that precipitates due to degassing of CO_2 is a function of pH since ^{13}C fractionates in the solute carbonate species and also into CO_2 gas. During degassing, the pH increases. Again, this is a Rayleigh problem which needs numerical integration and it can be done with PHREEQC-2 as shown in the symbolized input file of Example 2 where keywords RATES and KINETICS are invoked to degas CO_2, to precipitate calcite, and to find $\delta^{13}C$ (the full input file can be downloaded from www.xs4all.nl/~appt). Note here the flexibility of PHREEQC-2 for performing kinetic calculations in that multiple 'RATES' can be defined according to a specific hydrochemical or isotope problem.

```
# Example 2
# Degas CaHCO3 solution, precipitate calcite, find d13C...
SOLUTION 1
 Ca 5 charge; C(4) 10

RATES
 CO2(g) # d(CO2) / dt = -k * (P_aq - P_gas)
# parms 1= log(P_CO2)_gas. 2= reaction factor relative to calcite rate
 -start
  10 P_aq = sr("CO2(g)")
  20 dCO2 = parm(2) * (10^parm(1) - P_aq) * time
  30 save dCO2
  40 put(dCO2, 5)
 -end

 Calcite
# lines 10 to 200 from PHREEQC.DAT database, add line
  210 put(moles, 4) # ...store amount of calcite precipitate

 C13
# Distribute 13C among solute species 1= CO2aq, 2= HCO3-, 3=CO3-2
# and in calcite and CO2 gas.
 -start
# Define alpha's...
  10 aa_1_2 = exp-(9.866/TK - 24.12e-3) # Mook et al., 1974
  20 aa_3_2 = exp(-0.867/TK + 2.52e-3)  # Mook et al., 1974
  30 aa_cc_2 = exp(-4.232/TK + 15.1e-3) # Mook, 1986
  40 aa_g_2 = exp-(9.552/TK - 24.1e-3)  # Mook et al., 1974
# Find H12CO3- and H13CO3-...
  50 aH = act("H+")
  60 K1 = aH * act("HCO3-") / act("CO2") / act("H2O")
  70 K2 = aH * act("CO3-2") / act("HCO3-")
  80 m13C = m / (aa_1_2 * aH/K1 + 1 + aa_3_2 * K2/aH)
```

```
  90 m12C = (tot("C(4)")) / (aH/K1 + 1 +  K2/aH)
# and the ratio 13C/12C in HCO3-...
  100 R2 = m13C / m12C
# Fractionate 13C into calcite...
  110 d13C = aa_cc_2 * -get(4) * R2
# and in CO2(g)...
  120 d13C_g = aa_g_2 * -get(5) * R2
# Integrate...
  130 save d13C + d13C_g
# for printout and graphics...
  140 put(R2, 2);  180 put(d13C, 10);  190 put(d13C_g, 20)
 -end

C13_cc; -start; 10 save -get(10); -end    # ... store 13C in calcite
C13_g; -start; 10 save -get(20); -end     # ... store 13C in gas

KINETICS 1
 CO2(g); m0 0; -parm -3.5 0.001
 Calcite; m0 0; -parm 60 0.67
 C13; -formula C 0; m0 0.1112463e-3       # d13C = -10 permil
 C13_cc; -formula C 0; m0 0
 C13_g; -formula C 0; m0 0
 -step 1e-5 3 5 10 15 20 30 45 60 100 150 300 600 1e3 5e3
#... etc.
```

Figure 27.2 shows results for varying relative rates of carbon lost to the gas-phase and the calcite. For Figure 27.2A the two rates were set such that overall equilibrium with the final CO_2 pressure (in this case of $10^{-3.5}$ atm) and with calcite was reached at the same time. In this case, the pH increases rapidly to about 8 due to loss of CO_2, and subsequently more gradually because the precipitation of calcite keeps pace with the CO_2 loss. The $\delta^{13}C$ of the solution increases because the CO_2 loss to the gas phase occurs with a low $\delta^{13}C \approx -15‰$. The average $\delta^{13}C$ of the solution, the gas phase and the calcite increase during the approach to final equilibrium because the lighter isotope continues to be fractionated into the gas phase along the reaction path. Initially, $\delta^{13}C$ of the bicarbonate ion lies above the solution average because the lighter $CO_{2(aq)}$ forms a substantial part of total inorganic carbon (*TIC*), but as pH increases to 8.3, HCO_3^- becomes the major component of *TIC* and $\delta^{13}C$ of the solution and of HCO_3^- coincide. The line for calcite shows the increase of $\delta^{13}C$ in the *average* solid which changes from -7.5‰ to -5.4‰. However, the *actual* precipitate follows the line for bicarbonate and in the successive layers of the solid, $\delta^{13}C$ would range from -7.5‰ to -0.7‰.

Subtle changes take place if the rate for CO_2 loss is made much greater than for calcite precipitation, and this is probably the usual condition in field situations (Figure 27.2B). With a 100-fold increase of the rate 'CO2(g)', equilibrium among the solution and the gas-phase is virtually attained at all stages (the factor entered as parm(2) under KINETICS is increased from 0.001 to 0.1). Now, the pH increases initially to 8.9, and it decreases when protons are released during precipitation of calcite. The greater initial loss of carbon to the gas phase increases ^{13}C in solution and in calcite. Therefore, a slightly lighter solution and gas are found in the end.

Conversely, if the rate of calcite precipitation is increased 100-fold and the rate for CO_2 loss to the gas phase is kept the same as used for Figure 27.2A, the pH decreases initially (Figure 27.2C). Again, $\delta^{13}C$ in HCO_3^- increases, this time because the fraction of $CO_{2(aq)}$ increases. As a result, the gas phase becomes heavier, and the final solution and the calcite are both lighter than in the two previous cases. Thus, although the final, *chemical* composition of the solution is identical for all the paths, the *isotope* composition differs and may be a tracer for the actual pathway.

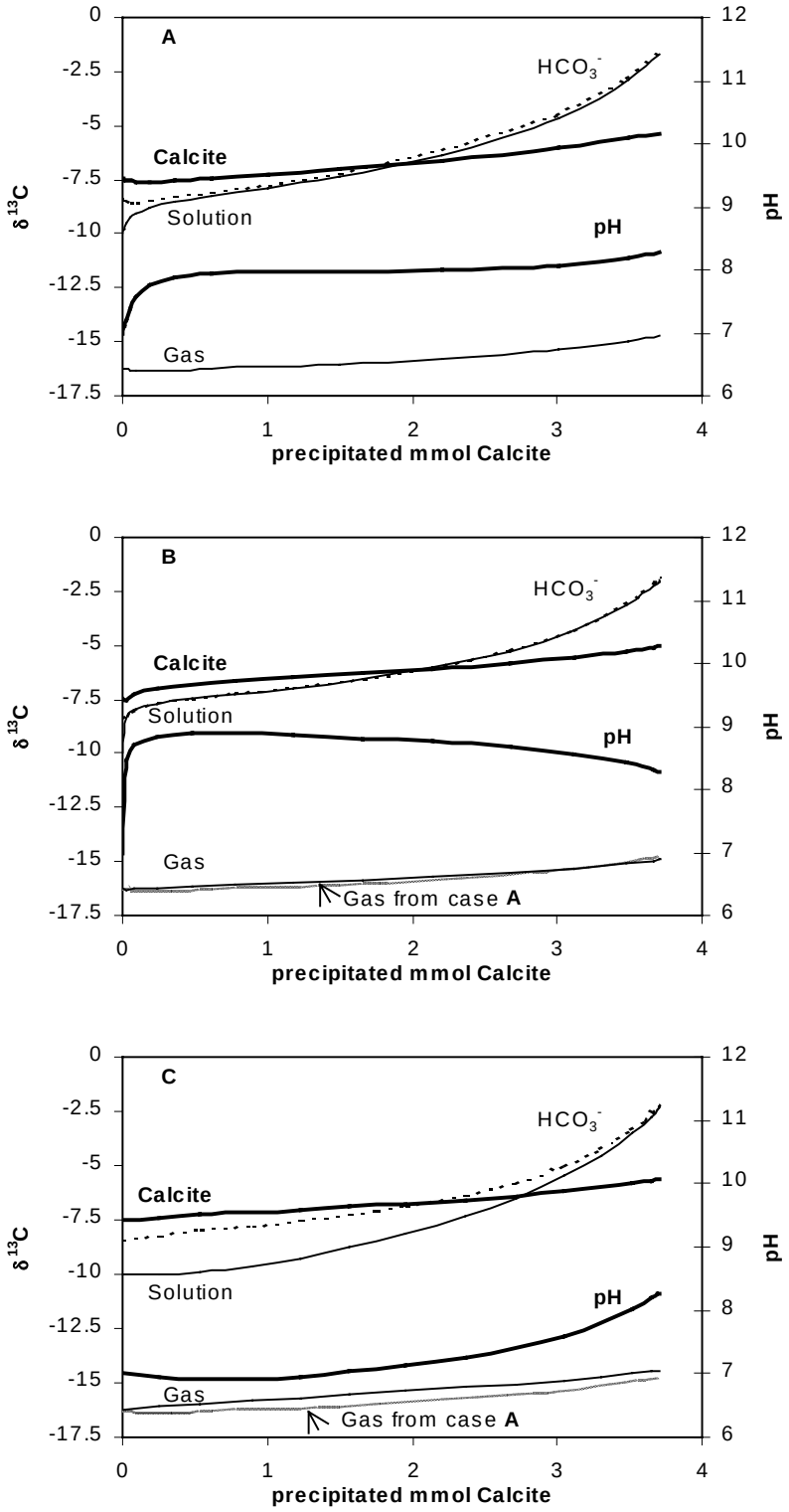

Figure 27.2. ^{13}C fractionation during degassing of 5 mM $Ca(HCO_3)_2$ solution. Initial pH = 7, solution $\delta^{13}C$ = -10‰. In A, the rates for degassing and for calcite precipitation approach equilibrium at the same pace. In B, the rate for CO_2 degassing is 100 fold greater, in C, the rate for calcite precipitation is 100 fold greater than in A, which leads to subtle changes in the isotope compositions. In B and C, the trace of $\delta^{13}C$ in gas from A is shown with a dotted line for comparison. Note that at high pH (case B), $\delta^{13}C$ of the solution (full line) and of HCO_3^- (dotted line) coincide.

27.2.2 Fractionation during precipitation and transport

For modeling ^{13}C fractionation during transport, the isotope should be introduced as a separate species in PHREEQC-2. For example, we imagine a flowline where a $NaHCO_3$ solution displaces $CaCl_2$ solution, and where cation exchange of Na^+ for Ca^{2+} induces supersaturation and precipitation of calcite. In Example 3, ^{13}C is introduced as a neutral species 'Ch', solute species for ^{13}C are not further detailed, but $H^{13}CO_3^-$ is calculated by simple fractionation among the H_2CO_3-HCO_3^--CO_3^{2-} species in a RATE that, again for space reasons is omitted but can be downloaded from www.xs4all.nl/~appt.

```
# Example 3
# Precipitate calcite during transport, find d13C...
SOLUTION_MASTER_SPECIES
 Ch Ch 0 1 1    # Ch is 13C
SOLUTION_SPECIES
 Ch = Ch; -log_k 0
SOLUTION 0
 pH 7 Calcite
 Na 10 charge; Ca 0.1
 C(4) 10;      Ch 0.1112463     # d13C = -10‰
SOLUTION 1-20
 Ca 5 charge;  Cl 10
END

KINETICS 1-100
 Calcite; m0 0; -parm 0.19 0.67
 C13; -formula Ch 1; m0 0

EXCHANGE 1-20
 X 0.1;      -equil 1
```

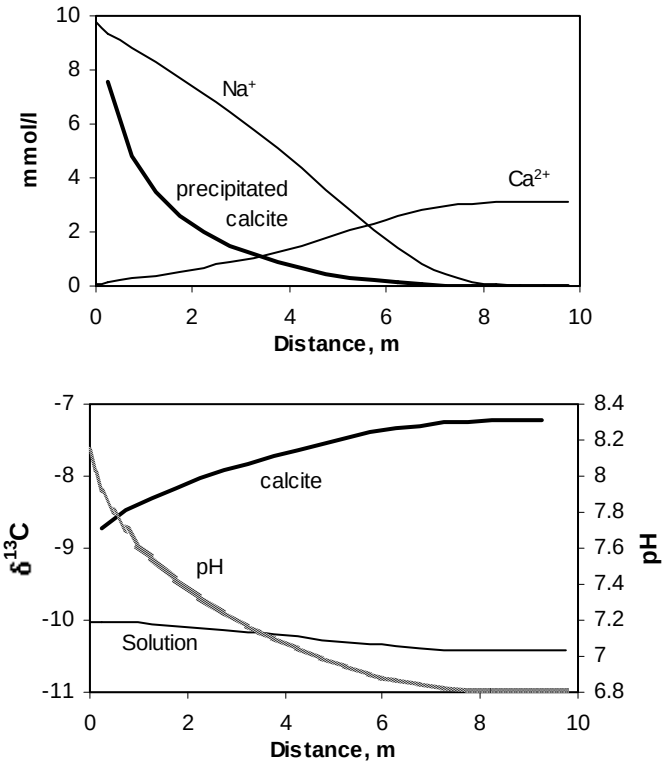

Figure 27.3. Calcite precipitation along a flowline, induced by cation exchange of Na^+ from injected solution for Ca^{2+} (upper graph); fractionation of ^{13}C into calcite and solution (lower graph).

```
TRANSPORT
 -cells 20;  -length 0.5
 -shifts 20; -timest 1.5768e6
 -diff 0;    -punch_frequency 20
END
```

The $NaHCO_3$ solution which enters the flowline has $\delta^{13}C$ = -10‰ determined by the concentrations of C(4) and Ch in SOLUTION 0. The exchanger along the flowline has an exchange capacity of 0.1 eq dm^{-3} and is equilibrated with solution 1, *i.e.* consists initially fully of CaX_2. Keyword TRANSPORT defines a flowline of 10 m that is traveled by the injected SOLUTION 0 in 1 year and resulting in a chemical and $\delta^{13}C$ profile shown in Figure 27.3.

Figure 27.3 indicates the decrease of the Na^+ concentration along the flowline due to exchange with Ca^{2+}. Part of the released Ca^{2+} precipitates in calcite, so that the sum of the cations (in meq dm^{-3}) also decreases. The fractionation of ^{13}C into calcite lightens the solution, but still, the calcite turns heavier along the flowline because the pH decreases in response to precipitation of calcite.

27.3 Fractionation due to diffusion

The different mass of two isotopes leads to different diffusion coefficients and a different distance traveled in a given time. For diffusion of a saline water from a constant reservoir into a sediment, Fick's second law can be integrated for the boundary conditions

$c(x, t) = c_i$, for $x > 0$, $t = 0$ and $x = \infty$, $t > 0$;

$c(x, t) = c_0$, for $x = 0$, $t > 0$

to give:

$$c(x,t) = c_i + (c_0 - c_i) \text{ erfc} \left(\frac{x}{\sqrt{4 D_e t}} \right) \quad (4)$$

where c is concentration (mol m^{-3}) as function of distance x (m), time t (s) and the effective diffusion coefficient D_e (m^2 s^{-1}). Erfc is the error function complement, 1 - erf. It can be calculated that the heavier isotope, which has a smaller diffusion coefficient than the lighter isotope, travels slower and that the salinizing solution in the sediment turns lighter at a larger distance for a given time (e.g. Clark and Fritz, 1997, fig. 6-24). On the other hand, if $c_i > 0$ and $c_0 = 0$, the freshening groundwater will become heavier. In both cases, the fractionation that is calculated from the ratio of the isotopes at some point is variable. Again, several effects may act together in a given field situation and we may need a numerical solution of the diffusion problem to calculate the isotope ratio at some point in time.

27.3.1 Cl-isotope diffusion

Beekman (1991) and Eggenkamp (1994) have measured $\delta^{37}Cl$ in the Markermeer lake bottom sediments where saline water diffusion took place for about 400 years from *A.D.* 1578 - 1932, followed by 55 years of back diffusion from the sediment into a fresh water lake from 1932 to 1987, the time of sampling. The Cl and $\delta^{37}Cl$ profile is displayed in detail in Figure 27.4. In the upper part of the boring, $\delta^{37}Cl$ shows a distinct positive bulge with a maximum of 0.89‰ at 2.4 m. Below 7 m, $\delta^{37}Cl$ is negative. When saline water diffuses in the sediment, ^{37}Cl is slightly slower than ^{35}Cl, and thus, negative $\delta^{37}Cl$ values are expected during the salt water diffusion stage. When the saline water diffuses out, ^{37}Cl is again slower than ^{35}Cl, and thus becomes enriched in the remaining salt water. Apparently, the enrichment results rapidly in a distinct, positive $\delta^{37}Cl$. The model lines in Figure 27.4 were obtained with a numerical model as will be dis-

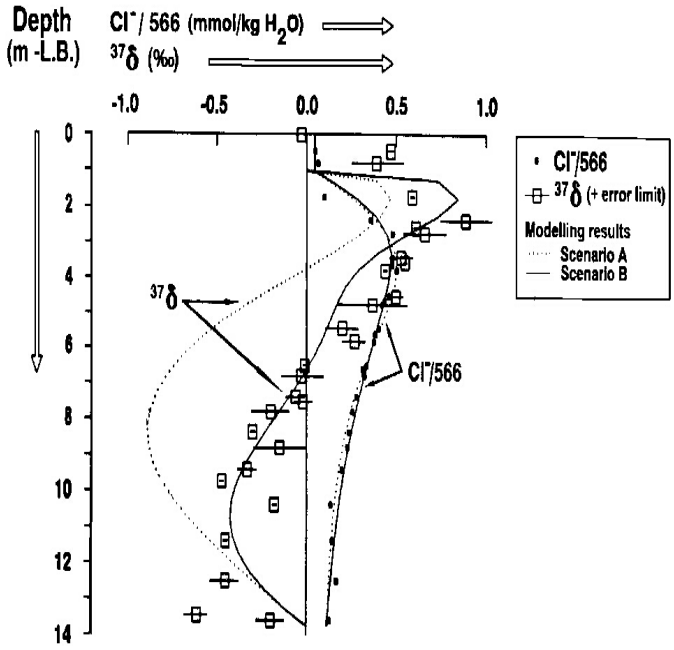

Figure 27.4. Profiles for Cl and δ^{37}Cl in the Markermeer sediment in 1987 (Beekman, 1991).

cussed shortly, but isotope fractionation during the stage of salt water diffusion can be calculated with Eq. (4) for the two isotopes with (slightly) different diffusion coefficients. Total chloride is then obtained by adding the two concentrations and δ^{37}Cl is calculated by dividing the two and normalizing to the standard ratio in seawater which contains 24.47% ^{37}Cl and 75.53% ^{35}Cl.

Thus, Figure 27.5 shows the calculated concentrations at the end of the saline stage in 1932, when the area was closed from the sea by a dam and became a fresh water lake. The Cl^- concentration shows the characteristic exponential trend of a diffusion profile, and does approximate the observed concentrations for depths greater than 4 m quite well. The model isotope ratio shows zero enrichment at both 0 and 18 m depth, the locations where seawater and initial water are found. In between, a minimum is calculated for δ^{37}Cl at 8 m. The calculated minimum is much greater than observed.

The stage of back diffusion of saline water can be calculated with PHREEQC-2 for the period

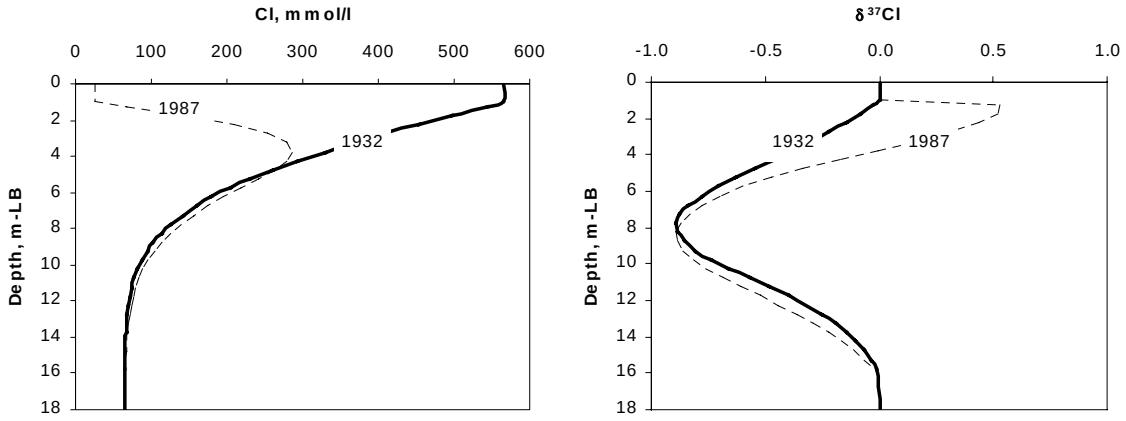

Figure 27.5. Calculated concentrations of Cl and δ^{37}Cl in the Markermeer sediment in 1932, at the termination of salt water diffusion over a period from 1578 till 1932. Dotted, light lines are for 1987, after fresh water diffusion in the period 1932-1987. These correspond with Scenario A in Figure 27.4.

from 1932 to 1987, but the program uses one value for the diffusion coefficient for all the species. Thus, the calculations must be done in two steps for the two isotopes, storing values for one isotope and subsequently calculating the other isotope with a modified diffusion coefficient. Total chloride and δ^{37}Cl are then obtained at the end of the second step. A quicker, but slightly less accurate alternative is to include a retardation for the heavier isotope, as illustrated in Example 4.

```
# Example 4
# Model delta 37Cl in Markermeer sediment.
SOLUTION_MASTER_SPECIES
 Clh Clh 0 1 1  # ... 37Cl
SOLUTION_SPECIES; Clh = Clh; log_k 0
SURFACE_MASTER_SPECIES
 Sor Sor    # ... sorber for retarding 37Cl
SURFACE_SPECIES
 Sor = Sor; -log_k 0
 Sor + Clh = SorClh; -log_k -102.9203     # log((R-1) / Sor) =
log(0.0012/10^100)
SOLUTION 1-30; Cl  49.0945; Clh 15.9055
SOLUTION 0;    Cl 427.4998; Clh 138.5002
END
    # Salt water diffusion until 1932 ...
SURFACE 1-200; Sor 1e100 1 1e100; -no_edl true; -equil 1
TRANSPORT
 -cells 30;         -length 0.5;  -shifts 1 0;  -boundary_conditions 1 1
 -diffusion_coefficient 8.4e-10;  -timest 1.14e10
END
    # Back diffusion, 1932 - 1987 ...
SOLUTION 0; Cl 18.8805; Clh 6.1195
TRANSPORT
 -timest 1.765e9
END
```

The retardation for ^{37}Cl amounts to $R = 1/0.9988 = 1.0012$. For linear retardation (R is constant), the equation is (Appelo and Postma, 1993):

$$R = 1 + \mathrm{d}q/\mathrm{d}c = 1 + q/c \tag{5}$$

where q is the sorbed concentration and c is the solute concentration in mol m^{-3}. Accordingly, the retardation can be modeled as linear sorption, with:

$$q/c = 0.0012 \tag{6}$$

Sorption can be included in PHREEQC-2 with keyword SURFACE and defined in the form of association reactions. A huge amount of sorber (10^{100} mol in example 4) and a very small association constant will keep the activity of the sorbing surface [Sor] constant irrespective of sorption of Clh. As a result, the mass action equation defined under keyword SURFACE_SPECIES as 'Sor + Clh = SorClh; -log_k -102.9203' has the same form as Eq. (6) and the product [Sor] $\cdot$ K = $10^{100}\times10^{-102.9203} = 10^{-2.9203} = 0.0012$ also gives the same constant.

The model results for 1987 are shown in Figure 27.5, and they correspond to 'Scenario A' in Figure 27.4. It can be seen that the Cl^- concentrations in the upper 4 m have decreased from 1932 till 1987, and that the computed concentrations well match the analyzed ones. However, the calculated δ^{37}Cl values do not agree with observations. The computed profile does show an increase of δ^{37}Cl in the upper meters, but the maximum is too small. Also, the minimum δ^{37}Cl remains too negative and the overall aspect suggests that the calculated profile has less ^{37}Cl than found in

the sediment cores. By doing exhaustive calculations and varying parameters, Beekman concluded that the bottom sediments were homogenized during storms and were gradually accumulating during the period of salt water diffusion. Thus, more ^{37}Cl was brought into the profile than would be the case with diffusion as the only process. The full lines in Figure 27.4 are for a sedimentation/erosion model ('Scenario B') which combines spasmodic events and calm periods in-between in which the concentration variations were smoothed out again (Beekman, 1981). It can explain the observed concentration variations, and also agrees well with the sedimentological observations. Scenario B can be calculated with PHREEQC-2 by adapting the time discretization and redefining the concentrations in the upper cells at given time intervals.

27.3.2 Fractionation limits

We started by noting that fractionation as result of diffusion would grow indefinitely with distance (Eq.. 4). However, Figure 27.5 shows that $\delta^{37}Cl$ is minimal at -8m and turns to 0‰ at -1 and -18m, as set by the boundary compositions. By varying the timelength of diffusion, it can be predicted that the minimum value for $\delta^{37}Cl$ = -0.88‰ remains constant, and only shifts to deeper levels at a constant ratio of x^2/t. Apparently, fractionation is limited when the two interdiffusing solutions contain both the isotopes. This does explain why $\delta^{37}Cl$ in groundwaters is generally smaller than ±1‰ (Eggenkamp, 1994; Clark and Fritz, 1997). Exceptional values down to -3.5‰ have been observed in extreme environments where gas hydrates provide a boundary composition with a very low $\delta^{37}Cl$ (Hesse et al., 2000).

It is of interest to consider the conditions where maximal fractionation can be expected. We take the quotient of the two isotope concentrations according to Eq. (4), differentiate the result with respect to x, and find the maximum when the derivative is zero. If the boundary solutions have δ = 0‰ and the ratio of the diffusion coefficients $D_h/D = f$, we obtain the minimal $\delta^{37}Cl$ (indicating maximal fractionation) at:

$$(\delta\ ^{37}Cl)_{min} = \left(\frac{1}{\sqrt{f}} \cdot \exp\left(\frac{x^2}{4\,D\,t} \cdot \frac{f\ -\ 1}{f} \right) - 1 \right) \cdot 1000 \qquad (7)$$

For the combination of $x^2/(4\,D\,t)$ where the minimum is located, $\delta^{37}Cl_{min}$ is a function of f and, although not explicitly noted in Eq. (7), also of the ratio of the total Cl concentrations and the δ's of the boundary solutions. Figure 27.6 shows how these factors influence the maximal attainable fractionation of Cl. As expected, the fractionation increases if the diffusion coefficients are more dissimilar and when the two solutions differ more in their Cl concentration. When seawater with 566 mM Cl and fresh water with 1 mM Cl interdiffuse, $\delta^{37}Cl_{min}$ = -3.88‰ for $D_{37}/D_{35} = f$ = 0.9988. The fractionation increases to -6.08‰ when a halite saturated solution diffuses into fresh water. When the ratio of the diffusion coefficients turns to 0.997, the maximal attainable fractionations are -9.68‰ and -15.15‰ for seawater and halite saturated water, respectively. The much smaller observed $\delta^{37}Cl$'s indicate that the ratio of the diffusion coefficients is likely to be close to 0.9988 or even nearer to 1. The small, *observed* fractionation in groundwaters also suggests that the ratio of the Cl concentrations of two adjacent, stagnant groundwaters is seldomly larger than 11, the ratio where $\delta^{37}Cl$ = -1‰ is attained. This is the ratio of seawater and a 50 mM Cl solution, and it may mark the maximum for many natural situations. Thus, the lack of Cl fractionation in groundwaters does probably not reflect that groundwater flow mixes the waters and reduces the concentration gradient but that fractionation during diffusion is small. In this respect, it should be noted that dispersion due to flow around heterogeneities does not fractionate the isotopes but only mixes waters.

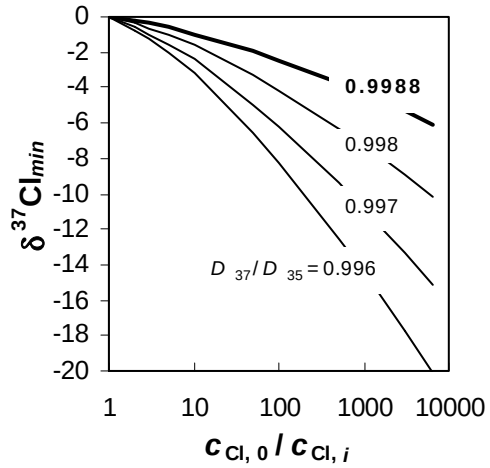

Figure 27.6. Maximal Cl fractionation (corresponding to *minimal* $\delta^{37}Cl$) as function of the ratio of the Cl concentrations in the two diffusing solutions and the ratio of the diffusion coefficients.

Eggenkamp and Coleman (1998) have analyzed $\delta^{37}Cl$ = -4‰ for Cl concentrations which are approximately twice higher than seawater in North Sea sediments. According to Figure 27.6, this requires for f = 0.9988, that the saline source water is at least 600 times more concentrated than the resident interstitial water. The calculated minimum for $\delta^{37}Cl$ in the analyses of Eggenkamp and Coleman coincides with a 4.6 times increase of the initial Cl concentration, from which $c_{Cl,\,i}$ ≈ 250 mM and $c_{Cl,\,0}$ ≈ 150 M are deduced. The latter value seems impossible (it amounts to 5.3 kg Cl dm^{-3}), and these samples should be investigated more closely to find the reasons for the anomalously low $\delta^{37}Cl$.

27.4 Conclusions

Isotope fractionation in natural systems can be calculated easily with the hydrogeochemical computer program PHREEQC-2. For Rayleigh processes the kinetic integrator can be used. Fractionation with diffusion can be simulated by calculating transport for each isotope, or, as illustrated, by calculating the lower diffusion velocity of the heavy isotope with the retardation equation. Fractionation of Cl isotopes in natural systems is small because the diffusion coefficients of ^{37}Cl and ^{35}Cl are nearly identical, and, fractionation into solid phases is very small (Eggenkamp, 1994). Fractionation of Cl is a function of the ratio of the chloride concentrations of the interdiffusing solutions. When the ratio is smaller than 11, the fractionation is limited to $\delta^{37}Cl$ < ±1‰.

27.5 References

Appelo, C.A.J. and Postma, D., 1993. *Geochemistry, groundwater and pollution*. Balkema, Rotterdam, 536 p.

Beekman, H.E., 1991. Ion chromatography of fresh- and seawater intrusion. PhD thesis, Free University Amsterdam, 198 p.

Bowers, T.S. and Taylor Jr, H.P., 1985. An integrated chemical and stable-isotope model of the origin of midocean ridge hot spring systems. J. Geophys. Res. 90, 12583-12606.

Clark, I. and Fritz, P., 1997. *Environmental isotopes in hydrogeology*. CRC Press, Boca Raton, Fl, 328 p.

Eggenkamp, H.G.M., 1994. The geochemistry of chlorine isotopes. PhD thesis, Univ. Utrecht, 150 p.

Eggenkamp, H.G.M. and Coleman, M.L., 1998. Heterogeneity of formation waters within and between oil fields by halogen isotopes. WRI-9, 309-312, Balkema, Rotterdam.

Hesse, R., Frape, S.K., Egeberg, P.K. and Matsumoto R., 2000. Stable isotope studies (Cl, O, and H) of interstitial waters from site 997, Blake Ridge gas hydrate field, West Atlantic 1. Proc. Ocean Drilling Program, Sci. Results, 164, 129-137.

Lasaga, A.C., 1998. *Kinetic theory in the earth sciences*. Princeton UP, 811 p.

Lee, M.K. and Bethke, C.M., 1996. A model of isotope fractionation in reacting geochemical systems. Am. J. Sci. 296, 965-988.

Parkhurst, D.L. and Appelo, C.A.J., 1999. User's guide to PHREEQC (version 2)-A computer program for speciation, batch-reaction, one-dimensional transport, and inverse geochemical calculations. US Geol. Survey, Water-Resour. Inv. Rep. 99-4259, 312 p.

{websites: www.xs4all.nl/~appt,
http://home.hccnet.nl/vincentpost/phreeqc.html
and wwwbrr.cr.usgs.gov/projects/GWC_coupled/phreeqc/index.html }

Thorstenson, D.C. and Parkhurst, D.L., 2002. Calculation of individual isotope equilibrium constants for implementation in geochemical models. Water Resour. Inv., in prep.

Valley, J.W. and Cole, D.R. (eds) 2001. Stable isotope geochemistry. Rev. Mineral. 43, 662 p.